JOURNAL OF SPACECRAFT AND ROCKETS
Vol. 29, No. 6, November-December 1992

Navier-Stokes Stall Predictions Using an Algebraic Reynolds-Stress Model

Lars Davidson*
Chalmers University of Technology, S-412 96 Gothenburg, Sweden
and
Arthur Rizzi†
FFA, The Aeronautical Research Institute of Sweden, S-16111 Bromma, Sweden

The paper presents results of a computational study of low-speed flow over an airfoil in stall. The code that solves the mean-flow equations is a rather standard explicit Runge-Kutta time-marching cell-centered finite volume technique using central differencing. The Baldwin-Lomax model failed to predict stall, and a standard k-ϵ transport model underpredicted the separation region in comparison with experiment. Only an algebraic Reynolds-stress model produced good agreement with the observed stall. The numerical treatment of the turbulent transport equations is novel. The k and ϵ equations are calculated implicitly using hybrid central/upwind differencing. A tridiagonal matrix procedure solves the resulting discretized linearized equations in both coordinate directions. This method for solving k and ϵ has proved to be very efficient and much more stable than the explicit solver used for the mean-flow equations. The combined approach therefore is semi-implicit. The influence of the explicit adding of the fourth-order numerical dissipation in the mean-flow equations is investigated, and it is shown that it has negligible effects on the calculated results.

Nomenclature

All variables have been nondimensionalized.

A_ϵ, A_ϵ, c_ℓ	= constants in one-equation model
C_{ij}, C_k	= convection of $\overline{u_i u_j}$ and k, respectively
C_p	= specific heat at constant pressure
c_μ, $c_{1\epsilon}$, $c_{2\epsilon}$, c_k, c_ϵ	= constants in k and ϵ equations
c_1, c_2, c_1', c_2'	= constants in algebraic stress model
D_{ij}, D_k	= diffusion of $\overline{u_i u_j}$ and k, respectively
E	= total energy per unit mass
e_x, e_y	= Cartesian unit vectors
F_I, F_V, F_T	= fluxes (inviscid, viscous, turbulent) in x direction
f	= damping function
F	= flux operator
G_I, G_V, G_T	= fluxes (inviscid, viscous, turbulent) in y direction
H	= stagnation enthalpy
$\mathcal{H}$	= flux vector
k	= turbulent kinetic energy
ℓ_μ, ℓ_ϵ	= turbulent length scales
M	= Mach number
n	= normal vector
n	= normal coordinate
S	= area
P_{ij}, P_k	= production of $\overline{u_i u_j}$ and k, respectively
p	= static pressure
Pr	= Prandtl number
Re	= Reynolds number
R_n	= turbulent Reynolds number
q_x, q_y	= conductive heat flux
T	= temperature
t	= time
U	= velocity vector
U	= velocity in x direction
V	= velocity in y direction
x, y	= Cartesian coordinates
δ	= finite difference operator
δ_{ij}	= Kronecker's δ
ϵ	= dissipation of k
ϵ_4	= coefficient for numerical dissipation
$\Phi_{ij,1}$ $\Phi_{ij,2}$	= pressure strain terms
$\Phi'_{ij,1}$, $\Phi'_{ij,2}$	= near-wall correction in terms of $\overline{u_i u_j}$
κ	= thermal conductivity coefficient
μ	= dynamic viscosity
ν	= kinematic viscosity
ρ	= density
$\rho\overline{u^2}$, $\rho\overline{uv}$, $\rho\overline{v^2}$	= Reynolds stresses
σ_k, σ_ϵ	= turbulent Prandtl numbers in k and ϵ equations
τ_{xx}, τ_{xy}, τ_{yy}	= viscous stresses
Ω	= volume

Subscripts

n	= normal to wall
s	= tangential to wall
t	= turbulent

Introduction

WE are concerned with calculating the flow around high-lift two-dimensional airfoils with the objective to be able to predict stall. A standard explicit Runge-Kutta time-marching cell-centered finite volume technique using central differencing[1,2] with fourth-order numerical nonhomogenous dissipation terms in all mean-flow equations stabilize the method.[3] The flow conditions of a case we are studying in detail are $Re = 2.1 \times 10^6$, $M = 0.15$, and angles of attack range from 0 to 19 deg. Work has been carried out improving the numerical scheme,[4] as well as implementing and testing different turbulence models such as the Baldwin-Lomax model and various k-ϵ models.[5,6] The main drawback in these efforts was that the separation zone near the trailing edge was much underpredicted compared with experiments, and when the angle of attack was increased the predicted lift coefficient increased even though the experiments show that stall should occur. It was believed that this failure of predicting stall could be due to inadequate turbulence models.

The turbulence on the suction surface of the profile is affected by the wall curvature and streamline curvature; near

Received March 17, 1992; revision received June 12, 1992; accepted for publication July 15, 1992.

*Assistant Professor, Thermo and Fluid Dynamics.

†Professor. Member AIAA.

and in the separation region, the streamwise normal Reynolds stress is much larger than that transversal one. None of the turbulence models tested so far can model these important phenomena, but overpredict the Reynolds stresses in the shear layer, and, consequently, predict the separation point too late and the separation zone much too small. This paper treats calculation of the flow just described using an explicit, compressible time-marching code and an algebraic Reynolds-stress model (ASM); this model has the ability to account for curvature effects on the turbulence, as well as for the strong nonisotropy of the turbulence. The paper presents results for stall that are in good agreement with the experiment.

From the Navier-Stokes equations an exact equation for the Reynolds stress $\overline{u_i u_j}$ can be derived. In the ASM, the transport (T_{ij} = convection-diffusion) of the Reynolds stresses is assumed to be proportional to that of the turbulent kinetic energy k. In this way an algebraic equation is obtained for $\overline{u_i u_j}$. This equation contains k and ϵ (= dissipation of k), which means that the equations for k and ϵ also have to be solved. The ASM, in contrast to standard k-ϵ models, does not make the eddy viscosity assumption, and thus does not assume isotropic turbulence.

The first part of the paper outlines the numerical method for solving the mean-flow equations, the second part presents the implementation of the ASM, and the final part presents the computed results together with a discussion including their interpretation. In the final part the influence of the numerical dissipation is also investigated.

Numerical Method

The numerical scheme we apply to solve the mean-flow equations belongs to the class of explicit Runge-Kutta schemes with central finite-volume differencing and adaptive artificial viscosity. By now the technique is rather standard and our particular one has been reported before. But for completeness, a brief description of the finite volume approach[1,2] taken to solve the Navier-Stokes equations written in Cartesian coordinates over a control volume Ω with boundary $\partial\Omega$ is given.

$$\frac{\partial}{\partial t}\iiint_{\Omega} U \, d\Omega + \iint_{\partial\Omega} \mathcal{H}(U)\cdot n \, dS = 0 \tag{1}$$

where the vector of state variables $U = (\rho\ \rho U\ \rho V\ \rho E)^T$ contains density ρ, x, and y components of mean-flow velocity U, V, and energy per unit mass E. The flux tensor $\mathcal{H}$ is composed of inviscid, viscous, and turbulent parts

$$\mathcal{H} = (F_I - F_V - F_T)e_x + (G_I - G_V - G_T)e_y \tag{2}$$

in the x- and y-coordinate directions, respectively.

The inviscid fluxes are given by

$$F_I = \begin{pmatrix} \rho U \\ \rho U^2 + p \\ \rho UV \\ \rho UH \end{pmatrix}, \qquad G_I = \begin{pmatrix} \rho V \\ \rho UV \\ \rho V^2 + p \\ \rho VH \end{pmatrix} \tag{3}$$

and the viscous and turbulent fluxes are given by

$$F_V + F_T = \begin{pmatrix} 0 \\ \tau_{xx} - \overline{\rho u^2} \\ \tau_{xy} - \overline{\rho uv} \\ U(\tau_{xx} - \overline{\rho u^2}) + V(\tau_{yx} - \overline{\rho uv}) - q_x \end{pmatrix}$$

$$G_V + G_T = \begin{pmatrix} 0 \\ \tau_{yx} - \overline{\rho uv} \\ \tau_{yy} - \overline{\rho v^2} \\ U(\tau_{xy} - \overline{\rho uv}) + V(\tau_{yy} - \overline{\rho v^2}) - q_y \end{pmatrix}$$

where $H = E + p/\rho$.

Components of the viscous stress tensor are

$$\tau_{xx} = \frac{2}{3}\mu\left(2\frac{\partial U}{\partial x} - \frac{\partial V}{\partial y}\right), \qquad \tau_{xy} = \tau_{yx} = \mu\left(\frac{\partial U}{\partial y} + \frac{\partial V}{\partial x}\right)$$
$$\tau_{yy} = \frac{2}{3}\mu\left(2\frac{\partial V}{\partial y} - \frac{\partial U}{\partial x}\right) \tag{4}$$

The heat-flux terms in the energy equation are not calculated with ASM, but the eddy-viscosity assumption is used, i.e.,

$$q_x = -\left(\frac{\mu}{Pr} + \frac{\mu_t}{Pr_t}\right)\frac{\partial T}{\partial x}, \qquad q_y = -\left(\frac{\mu}{Pr} + \frac{\mu_t}{Pr_t}\right)\frac{\partial T}{\partial y}$$

where the turbulent viscosity is obtained from k and ϵ as

$$\mu_t = c_\mu \rho(k^2/\epsilon)$$

The value of the Prandtl number $Pr = \mu C_p/\kappa$ was taken as a constant 0.72, and Pr_t was set to 0.9 (constant) for the turbulent flow solutions presented in this paper. The laminar viscosity μ is calculated using the Sutherland formula.

The usual finite-volume approximations have been made to Eq. (1) for a quadrilateral cell of volume Ω

$$\frac{d}{dt}U_\Omega = -\frac{1}{\Omega}\iint_{\partial\Omega} \mathcal{H}(U)\cdot n \, dS$$
$$= -\frac{1}{\Omega}\sum_{f=1}^{4} \mathcal{H}(U)_f \cdot S_f = \sum_{f=1}^{4} F(U)_f \tag{5}$$

Space Discretization

The scheme for the inviscid terms is a cell-centered finite volume discretization in space that is fully conservative (at steady state with local time stepping). The flux at a cell face is computed as the flux of the average of the two state variables to the left and right of the face. An artificial smoothing term F_N is added that stabilizes this discretization. The proposed modification of Swanson and Turkel[3] is used which takes the cell-aspect ratio into account through the directional convective local time step t^d, and which decreases F_N in the boundary layers by scaling F_N with the local Mach number M. The semidiscrete form of the scheme applied to Eq. (5) in one space dimension illustrates these points

$$\frac{d}{dt}U_j = \delta F_j = F_{j+\frac{1}{2}} - F_{j-\frac{1}{2}} \tag{6}$$

where

$$F_{j+\frac{1}{2}} = F\left(\frac{U_j + U_{j+1}}{2}\right) - \epsilon_4 CFL\,\delta_j\left[\frac{M}{M_\infty}\frac{1}{t_j^d}\delta_j^2\right]U_j \tag{7}$$

where the second term consists of the numerical dissipation F_N^j, which is a fourth-difference term.

It must be pointed out that the numerical smoothing terms have to be treated correctly near boundaries to maintain good convergence and to keep the variations in entropy small.[1,2]

The viscous terms are computed in a two-step procedure. First, the gradients in the cell are formed by the gradient theorem, then the viscous terms are computed, and the viscous flux tensor is found. Second, averaging this tensor in Eq. (7) over the cell face gives the numerical flux at the center of the face for use in Eq. (5).

Time Integration

After space discretization, Eq. (5) becomes

$$\frac{d}{dt}U_{ij} = \sum_{f=1}^{4} F(U)_f = \delta F_{ij} = (\delta_i + \delta_j)F_{ij} \tag{8}$$

where Eqs. (6) and (7) imply the meaning of the difference operators. The resulting semidiscrete system of ordinary differential equations is solved by a standard explicit four-stage Runge-Kutta time integration with local time stepping. The standard four-stage scheme applied to Eq. (8) is

$$U_{ij}^{(1)} = U_{ij}^{n} + \alpha_1 \Delta t \delta F_{ij}^{n} \tag{9a}$$

$$U_{ij}^{(2)} = U_{ij}^{(1)} + \alpha_2 \Delta t \delta F_{ij}^{(1)} \tag{9b}$$

$$U_{ij}^{(3)} = U_{ij}^{(2)} + \alpha_3 \Delta t \delta F_{ij}^{(2)} \tag{9c}$$

$$U_{ij}^{n+1} = U_{ij}^{(3)} + \alpha_4 \Delta t \delta F_{ij}^{(3)} \tag{9d}$$

where the superscripts identify the temporal level, and the multistage coefficients are $\alpha_1 = 1/3$, $\alpha_2 = 4/15$, $\alpha_3 = 5/9$, and $\alpha_4 = 1$.

Boundary Conditions

Appropriate boundary conditions are required on the airfoil surface, at the far field, and at the periodic boundaries. The usual no-slip boundary conditions have been enforced on the airfoil. The condition for pressure on the airfoil surface has been set by second-order extrapolation from the field values and the wall is considered to be adiabatic. The far field has been assumed to be inviscid and treated by either setting or extrapolating the locally one-dimensional Riemann invariants. The trailing edge is sharp. The boundary conditions on the periodic line are straightforward.

Turbulence Model

Algebraic Stress Model

The form of the exact Reynolds-stress equation can be derived from the incompressible Navier-Stokes equations. Since the Mach number in the present case is low (= 0.15), density fluctuations have been neglected.

An ASM is a simplified Reynolds-stress model, where the transport (convective and diffusive) of the Reynolds stresses $\overline{u_i u_j}$ is related to that of the turbulent kinetic energy k, i.e.,

$$T_{ij} \equiv C_{ij} - D_{ij} = (\overline{u_i u_j}/k)(C_k - D_k) \tag{10}$$

Some algebraic manipulation[7] gives the expression for the standard algebraic Reynolds-stress model, which—using Cartesian velocity components—reads[8]

$$\overline{u_i u_j} = \frac{2}{3}\delta_{ij}k + \frac{k}{\epsilon}\frac{(1-c_2)(P_{ij} - \frac{2}{3}\delta_{ij}P_k) + \Phi'_{ij,1} + \Phi'_{ij,2}}{c_1 + P/\epsilon - 1} \tag{11}$$

where the standard modelization of the pressure-strain correlation terms[8] has been used. The near-wall correction terms and the production term have the form

$$\Phi'_{ij,1} = c_1'(\epsilon/k)(\overline{u_n^2}\delta_{ij} - \tfrac{3}{2}\overline{u_n u_i}\delta_{nj} - \tfrac{3}{2}\overline{u_n u_j}\delta_{ni})f(\ell_t/x_n)$$

$$\Phi'_{ij,2} = c_2'(\Phi_{nn,2}\delta_{ij} - \tfrac{3}{2}\Phi_{ni,2}\delta_{nj} - \tfrac{3}{2}\Phi_{nj,2}\delta_{ni})f(\ell_t/x_n)$$

$$P_{ij} = -\overline{u_i u_k}\frac{\partial U_j}{\partial x_k} - \overline{u_j u_k}\frac{\partial U_i}{\partial x_k}$$

The f function is a damping function that reduces the effect of the wall correction with increasing distance x_n (n denotes normal direction), and which has the form $f = k^{3/2}/(2.55 x_n \epsilon)$. The constants are standard ones[8]: $c_1 = 1.8$, $c_1' = 0.5$, $c_2 = 0.6$, and $c_2' = 0.3$.

Equation (11) is a 3×3 matrix system. Because of the stiff response of the coupled equations for the algebraic Reynolds stresses in Eq. (11) to the mean velocity field, the system is reduced to a 2×2 system transferring the shear stresses to the right-hand side. When solving the normal stresses implicitly from the obtained 2×2 system, special care must be taken to ensure that they stay positive. Note that the near-wall correction terms are in simplified form. For more details, see Refs. 7 and 9.

k and ϵ Equations

Since k and ϵ appear in the equation for the Reynolds stresses $\overline{u_i u_j}$ in Eq. (11), the equations for k and ϵ also have to be solved. The standard k and ϵ equations in the ASM have the form:

$$\frac{\partial}{\partial x_j}(\rho U_j k) = \frac{\partial}{\partial x_j}\left[\left(\mu + c_k \rho \overline{u_j u_m}\frac{k}{\epsilon}\right)\frac{\partial k}{\partial x_m}\right] + P_k - \rho\epsilon \tag{12}$$

$$\frac{\partial}{\partial x_j}(\rho U_j \epsilon) = \frac{\partial}{\partial x_j}\left[\left(\mu + c_\epsilon \rho \overline{u_j u_m}\frac{k}{\epsilon}\right)\frac{\partial \epsilon}{\partial x_m}\right] + \frac{\epsilon}{k}(c_{1\epsilon}P_k - c_{2\epsilon}\rho\epsilon) \tag{13}$$

$$P_k = -\rho\overline{u_i u_j}\frac{\partial U_i}{\partial x_j}$$

$$c_k = 0.22, \qquad c_\epsilon = 0.17, \qquad c_{1\epsilon} = 1.44, \qquad c_{2\epsilon} = 1.92$$

Normally, the diffusion terms in the k and ϵ equations have little influence on the flowfield. Calculations modeling these diffusion terms using the eddy-viscosity assumption were also carried out, but no noticeable changes in the calculated results were observed.

Initially, attempts were carried out to solve the k and ϵ equations explicitly using the existing Runge-Kutta solver. However, no stable, convergent solution was obtained. The main cause for these problems was probably the large source terms. To remedy these stability problems, a semi-implicit solver was implemented for solving k and ϵ.[5,10,11]

Near-Wall Treatment

Near the walls the one-equation model by Wolhshtein,[12] modified by Chen and Patel,[13] is used. In this model, the standard k equation is solved; the diffusion term in the k equation is modeled using the eddy-viscosity assumption. The turbulent length scales are prescribed as

$$\ell_\mu = c_\ell n[1 - \exp(-R_n/A_\mu)], \quad \ell_\epsilon = c_\ell n[1 - \exp(-R_n/A_\epsilon)] \tag{14}$$

(n is the normal distance from the wall) so that the dissipation term in the k equation and the turbulent viscosity are obtained as

$$\epsilon = k^{3/2}/\ell_\epsilon, \qquad \mu_t = c_\mu \rho \sqrt{k}\,\ell_\mu \tag{15}$$

The Reynolds number R_n and the constants are defined as

$$R_n = \sqrt{k}n/\nu, \quad c_\mu = 0.09, \quad c_\ell = \kappa c_\mu^{-3/4}, \quad A_\mu = 70, \quad A_\epsilon = 2c_\ell$$

The one-equation model is used near the walls (for $R_n \le 2.5 \times 10^2$; the matching line is chosen along a preselected grid line), and the ASM together with the standard k and ϵ equations in the remaining part of the flow. Since the ASM is not valid near the wall, the Reynolds stresses are here computed using the Boussinesq assumption, i.e.,

$$\overline{\rho u_i u_j} = -\mu_t\left(\frac{\partial U_i}{\partial x_j} + \frac{\partial U_j}{\partial x_i} - \frac{2}{3}\delta_{ij}\frac{\partial U_m}{\partial x_m}\right) + \frac{2}{3}\delta_{ij}\rho k \tag{16}$$

where μ_t is calculated using Eq. (15). The matching of the one-equation model and the k and ϵ equations does not pose any problems but gives a smooth distribution of μ_t and ϵ across the matching line. However, the matching of the ASM and the one-equation model gives rise to noncontinuity in the Reynolds stresses across the matching line. The one-equation model gives more or less isotropic normal Reynolds stresses

according to Eq. (16), whereas ASM gives highly nonisotropic Reynolds stresses, which result in a jump in the profiles of $\overline{u^2}$ and $\overline{v^2}$ across the matching line. Also the $\overline{uv}$ profile is nonsmooth across the matching line due to an inconsistency between the one-equation model (or the k-ϵ model) and the ASM. To illustrate this, a boundary-layer flow is chosen where

$$f = 1, \qquad P_k \simeq \epsilon, \qquad P_k = -\overline{uv}\frac{\partial U}{\partial y}$$

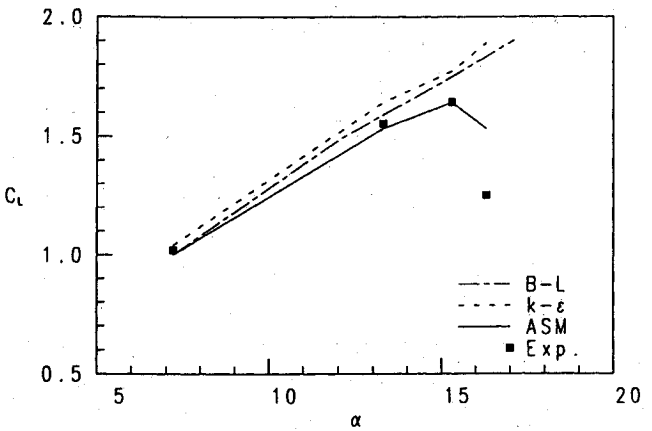

Fig. 1 Calculated lift coefficient C_L vs angle of incidence α compared with experiments. Three different turbulence models have been used: ASM, two-layer k-ϵ, and Baldwin-Lomax.

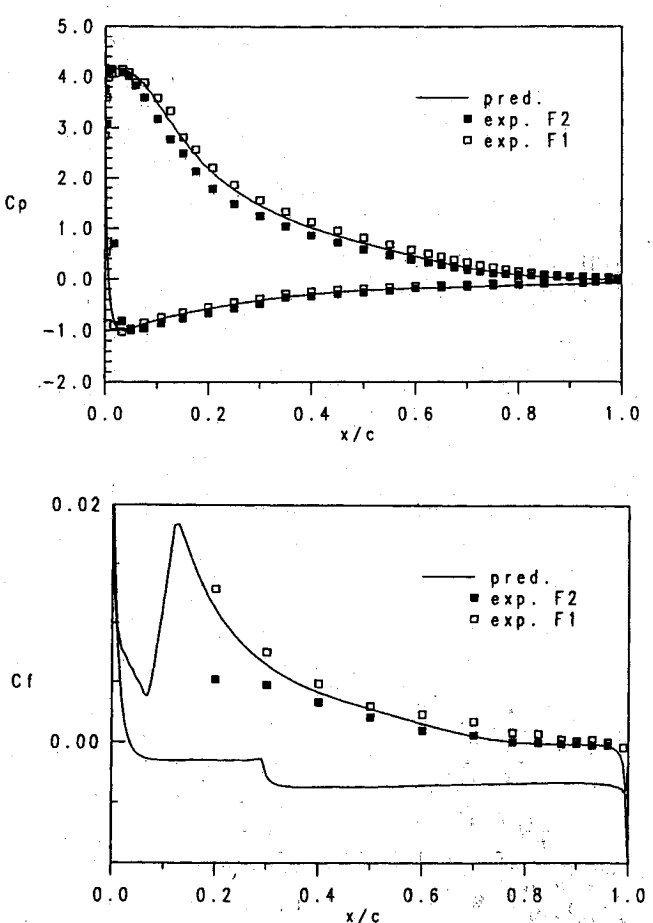

Fig. 2 Comparison between calculated (using ASM) and experimental surface pressure C_P and skin friction C_F. $\alpha = 13.3$ deg ——: predictions; symbols: experiments (□: F1 wind tunnel, and ■: F2 wind tunnel).

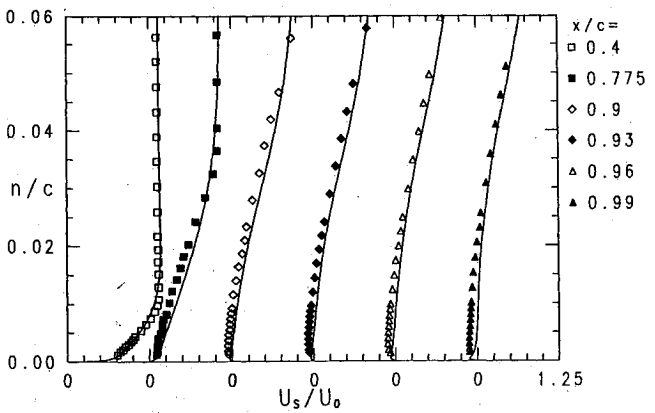

Fig. 3 U_s/U_0 on the suction side. Solid lines: predictions; and markers: experiments.

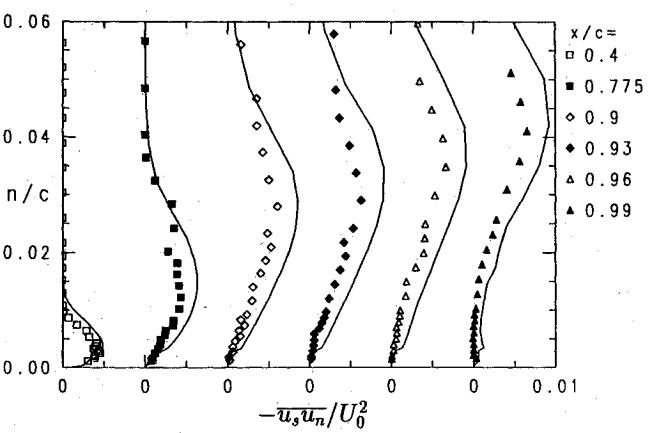

Fig. 4 Reynolds shear stresses $-\overline{u_s u_n}/U_0^2$ on the suction side. Solid lines: predictions; and markers: experiments.

so that Eq. (11) gives

$$\overline{v^2} = \frac{2}{3}k\frac{c_1 - 1 + c_2(1 - 2c_2')}{c_1 + 2c_1'} \tag{17}$$

$$-\overline{uv} = \frac{1 - c_2 + \frac{3}{2}c_2c_2'}{c_1 + \frac{3}{2}c_1'}\overline{v^2}\frac{k}{\epsilon}\frac{\partial U}{\partial y} \tag{18}$$

Inserting values for the constants gives $-\overline{uv} = 0.065k^2/\epsilon\partial U/\partial y$. The coefficient 0.065 should be compared with $c_\mu = 0.09$, which the k-ϵ model as well as the one-equation model gives.

The matching problems just discussed do not seem to create any serious problems: the equations remain stable, despite small jumps in the Reynolds-stress profiles.

Results and Discussion

A 353 × 65 C-mesh, generated by Palicot,[14] has been used. The near-wall nodes are located at $y^+ \simeq 1$, and 7 to 10 nodes in the normal direction are situated in the region $0 \le y^+ \le 20$.

The calculated results (for more details, see Ref. 7) are compared with experimental data taken from Refs. 15 and 16. The Reynolds number and the Mach number are 2.1×10^6 and 0.15, respectively. Measurements have been carried out in two wind tunnels, F1 and F2. In the F1 wind tunnel, global characteristics such as friction coefficients and surface pressures were measured. The flowfield was studied in more detail in the F2 wind tunnel, where mean velocity profiles and Reynolds stresses were measured using a three-component laser Doppler velocimetry-system. The blockage effect in the F2 tunnel was more important than in the F1 tunnel, leading to three-dimensional effects for $\alpha \ge 13$ deg.

The main motivation for implementing an ASM was that using other lower-order turbulence models such as Baldwin-

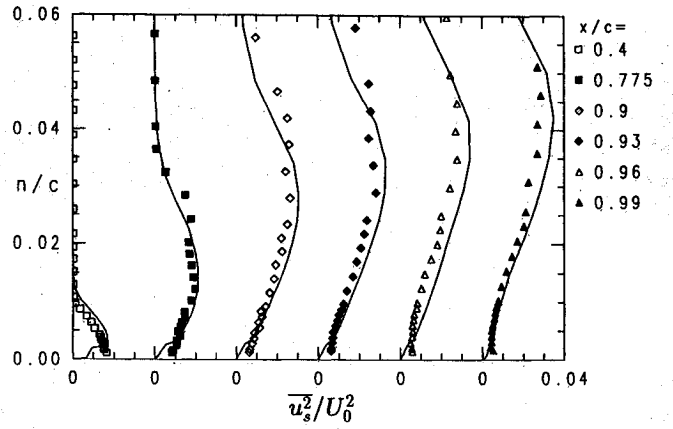

Fig. 5 Reynolds normal stresses $\overline{u_s^2}/U_0^2$ on the suction side. Solid lines: predictions; and markers: experiments.

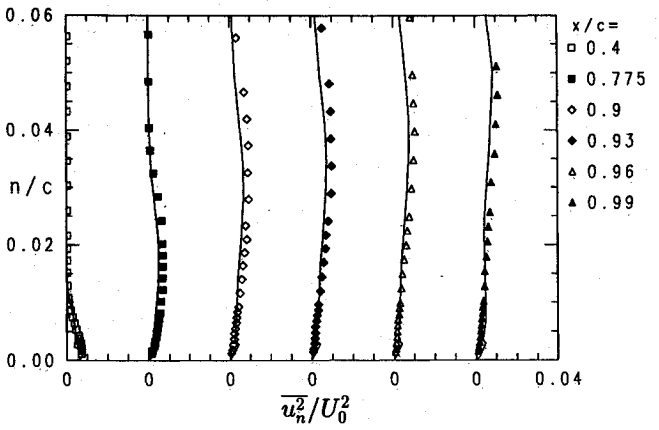

Fig. 6 Reynolds normal stresses $\overline{u_n^2}/U_0^2$ on the suction side. Solid lines: predictions; and markers: experiments.

Lomax or k-ϵ models, the separation was predicted much too late and the separation zone much too small, and, consequently, no stall was predicted. In Fig. 1, the predicted lift coefficients using the Baldwin-Lomax[14] and the k-ϵ model[5,6] are compared with experimental data.[15,16] It is seen that the predicted C_L using the Baldwin-Lomax model and the k-ϵ model show no tendency to decrease for increasing angle of attack, whereas the ASM does predict a decrease in C_L at approximately $\alpha = 16$ deg, which is in agreement with experiments.

The calculated results using ASM are presented below in more detail for $\alpha = 13.3$ deg. The main characteristics of the flow are presented in the form of c_p and c_F curves in Fig. 2. It can be seen that the calculated surface pressure and surface friction agree very well with the experimental values. The U_s velocities and the Reynolds stresses on the suction side of the airfoil are presented in Figs. 3–6. Note that in Figs. 3–6 an orthogonal s-n coordinate system is used. The s coordinate is tangential to the airfoil, with origin on the surface. The U_s velocities on the profile are well predicted. As separation is approached, it is seen that the predicted U_s profiles follow the experimental ones, the profiles getting progressively less full, and that an inflection point in the profiles appears. It can also be seen from Figs. 5 and 6 that the anisotropy in the normal Reynolds stresses gets more and more pronounced as the trailing edge is approached. Small kinks in the Reynolds stresses are visible at the matching line between the ASM and the one-equation model.

In boundary-layer flow, the only term that contributes to the production term in the k and ϵ equations is $-\overline{u_s u_n}\partial U_s/\partial n$. Thompson and Whitelaw[17] found that near the separation point, as well as in the separation zone, the production term $-(\overline{u_s^2} - \overline{u_n^2})\partial U_s/\partial s$ was of equal importance. In Fig. 7 these terms are presented. At $x/c = 0.2$, the production term due to the normal stresses is not very large (at the most, 10% of that due to the shear stress). However, in the separation region the two terms are of equal importance (see Fig. 7c). In Fig. 7, the dissipation is also presented, and it is seen that production and dissipation balance each other at $x/c = 0.2$, but that near the separation point and especially in the separation region, this is not the case. The production term using the eddy-viscosity assumption $\nu_t(\partial U_s/\partial n)^2$ (the contribution from the normal stresses is negligible) is also included in Fig. 7, which should be compared with $-\overline{u_s u_n}\partial U_s/\partial n$. Note that this is a comparison between the shear stress obtained with the ASM and that obtained using the eddy-viscosity assumption $\overline{u_s u_n} = -\nu_t \partial U_s/\partial n$. It can be seen that the shear stress obtained using the eddy-viscosity assumption is considerably larger than that obtained using the ASM. This is because the ASM accounts for the damping of the shear stress and the Reynolds stress normal to the wall; for boundary-layer flow the ASM yields, with

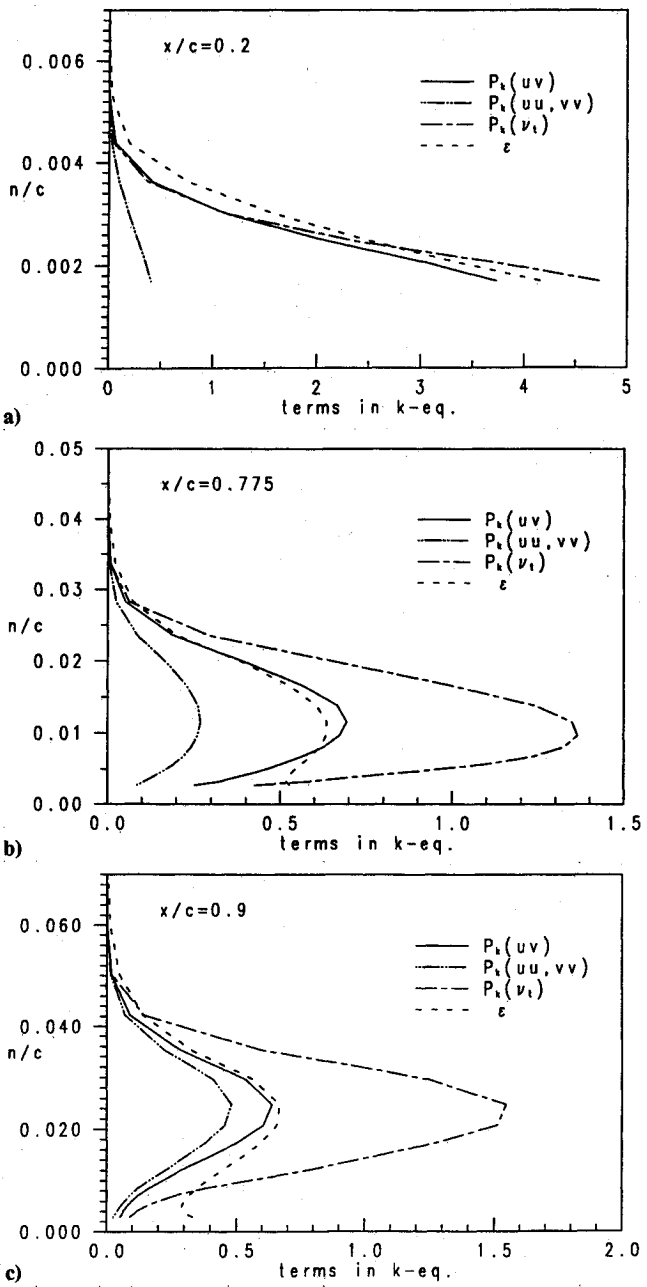

Fig. 7 Calculated terms in the k equation. Production due to shear stresses, $-\overline{u_s u_n}\partial u_s/\partial n$; production due to normal stresses, $(\overline{u_n^2} - \overline{u_s^2})\partial U_s/\partial s$; production using eddy-viscosity assumption, $\nu_t[\partial U_s/\partial n]^2$; dissipation in k equation, ϵ: a) $x/c = 0.2$; b) $x/c = 0.775$; and c) $x/x = 0.9$.

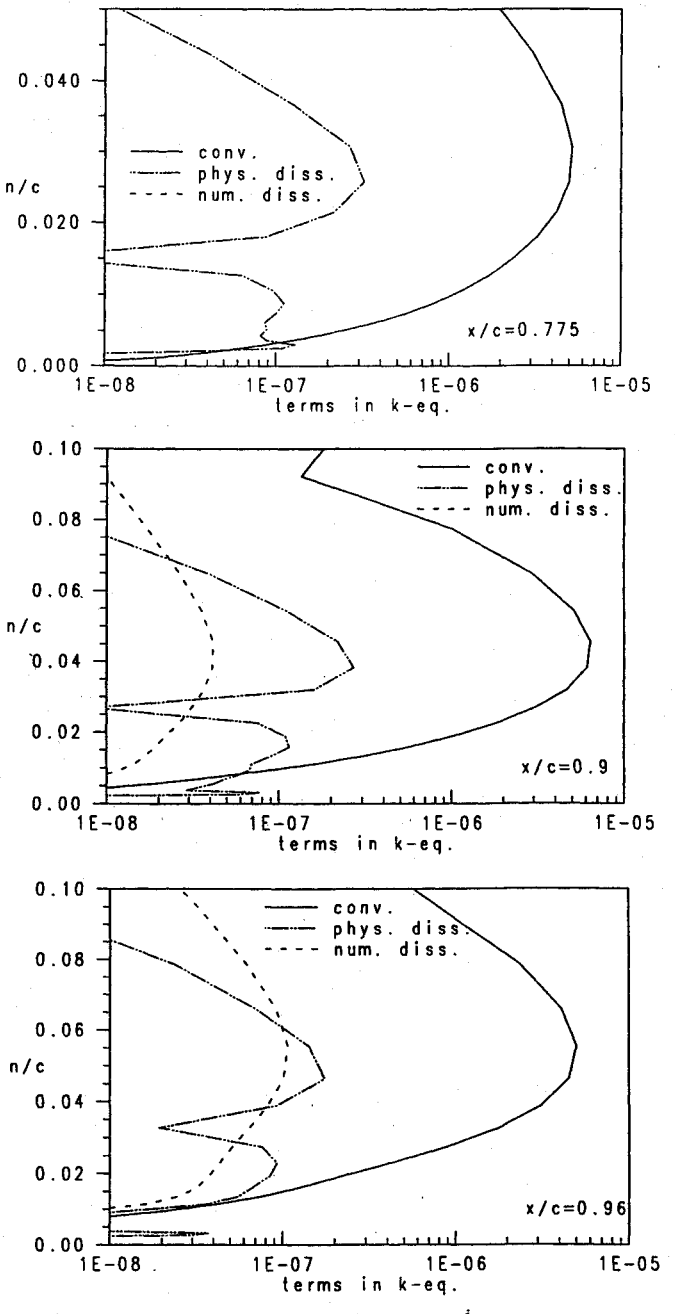

Fig. 8 Magnitude of the numerical dissipation F_N^j in the ρU equation compared with the magnitude of the convective term C^j (excluding the pressure) and the diffusive term D^j (viscous and turbulent): a) $x/c = 0.775$; b) $x/c = 0.9$; and c) $x/c = 0.96$.

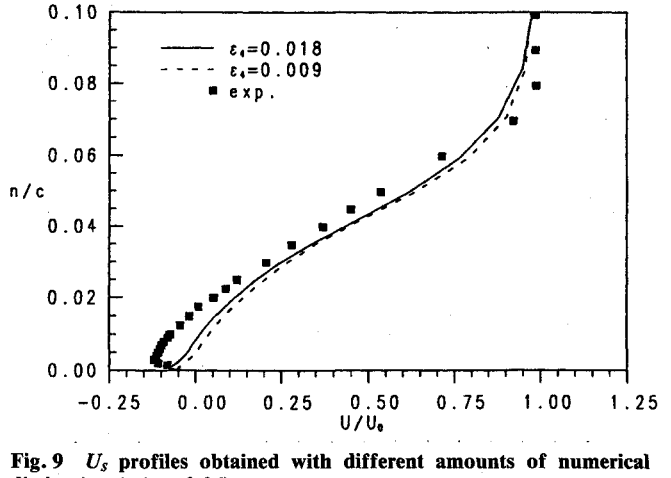

Fig. 9 U_S profiles obtained with different amounts of numerical dissipation ($x/c = 0.96$).

damping, a c_μ coefficient of 0.065 [see Eq. (17)], which is 28% smaller than the c_μ used in k-ϵ models.

Finally, a few words about computer requirements. Of course the ASM is more expensive than a k-ϵ model or a Baldwin-Lomax model. The increase in computing time per time step is modest (approximately 10% higher than the k-ϵ model), but the total CPU time increases considerably due to two facts: a rather complicated startup procedure, and because the computed solution using the ASM—contrary to the other models—exhibits a large separation zone, which means that the flow becomes more complicated and thus requires more computing time. To ensure a stable solution process, a rather complicated startup process is used. First, the flow is computed with the Baldwin-Lomax model. Then, during 500–1000 time steps, the mean flowfields are frozen, and the k and ϵ transport equations together with the algebraic equations for the Reynolds stresses are solved. After that, the complete equation system is solved. Normally, the complete equation system converges after 20,000 time steps.

Influence of the Numerical Dissipation

When using advance turbulence models, it is important that the numerical discretization method is accurate and that the numerical dissipation is smaller than the physical diffusion. In the present study, central differencing together with explicit adding of numerical dissipation is used. Even if the more recent total variation diminishing schemes, which recently have been used together with transport turbulence models such as the k-ϵ model (see, e.g., Ref. 18), probably are more accurate and less diffusive than the present scheme, the present scheme has one undisputable advantage: it is controllable and measurable. Since the numerical dissipation is added explicitly, it can easily be compared with the other terms in the equations. In Fig. 8, the numerical dissipation [Eq. (7)] in the ρU equation is compared with the convective and diffusive terms. The numerical dissipation is negligible compared with the physical diffusion as long as the flow remains attached; see Fig. 8a. However, in the separation region the numerical dissipation becomes more important. At $x/c = 0.9$, it reaches values of approximately 50% of the physical diffusion. Further downstream (at $x/c = 0.96$), it becomes, close to the wall, of comparable importance as the physical diffusion.

The coefficient ϵ_4 in the numerical dissipation term [see Eq. (7)] was set to $\epsilon_4 = 0.018$. A value of $\epsilon_4 = 0.009$ was also tested. This resulted in only little change in the overall flow characteristics: the lift coefficient C_L increased by 0.6%, and the oscillations in the pressure field near the trailing edge increased. In Fig. 9, two velocity profiles obtained with $\epsilon_4 = 0.018$ and 0.009 are compared for $x/c = 0.96$, and it can be seen that the numerical dissipation does not have any large effect on the predicted velocity profile.

Conclusions

The flow around a two-dimensional high-lift airfoil has been calculated using an algebraic stress turbulence model. (ASM), which has been implemented into an existing explicit Runge-Kutta finite volume code. To obtain stable and convergent solutions the k and ϵ equations—which are calculated when using ASM—are solved with an implicit solver.[5,10,11]

When using advance turbulence models, it is important to verify that the numerical dissipation does not have any adverse effects on the accuracy; it has been shown that the numerical dissipation has negligible influence on the flowfield.

As the ASM is only valid for fully turbulent flow, it has been matched with a one-equation model close to the wall. ($y^+ \leq 50$). This turbulence model has been shown to be able to predict stall for an angle of attack of 16 deg, which is in agreement with experiments. Earlier work[5,6] has shown that k-ϵ models are not able to predict stall, and that these models overpredict the shear stress, and consequently predict separation too late and separation regions too small. The main reasons for the superiority of the ASM are believed to be its

ability of taking into account the influence of streamline curvature[19] and the large difference in the normal Reynolds stresses.

Acknowledgment

The free computer resources at CERFACS, Toulouse, France—where most of the work was carried out—are gratefully acknowledged.

References

[1]Rizzi, A., and Müller, B., "Large-Scale Viscous Simulation of Laminar Vortex Flow Over a Delta Wing," *AIAA Journal,* Vol. 27, No. 7, 1989, pp. 833–840.

[2]Müller, B., and Rizzi, A., "Modeling of Turbulent Transonic Flow Around Aerofoils and Wings," *Communications in Applied Numerical Methods,* Vol. 6, Oct. 1990, pp. 603–613.

[3]Swanson, R. C., and Turkel, E., "Artificial Dissipation and Central Difference Schemes for the Euler and Navier-Stokes Equations," AIAA Paper 87-1107, Jan. 1987.

[4]Gendre, P., "Computation of Low Speed Flow Around High-Lift Single Element Airfoils With a 2D-Navier-Stokes Solver," *Proceedings of the Second World Congress on Computational Mechanics,* Vol. 1, Stuttgart, Germany, Aug. 1990, pp. 202–205.

[5]Davidson, L., "Implementation of a Semi-Implicit k-ϵ Turbulence Model in an Explicit Runge-Kutta Navier-Stokes Code," Centre Européen de Recherche et de Formation Avancée en Calcul Scientifique (CERFACS), TR/RF/90/25, Toulouse, France, May 1990.

[6]de Cambray, E., "Evaluation d'un modéle k-ϵ dans un code Navier-Stokes," Thése DEA, Centre Européen de Recherche et de Formation Avancée en Calcul Scientifique (CERFACS), TR/RF/90/25, Toulouse, France, Sept. 1990.

[7]Davidson, L., "Predicting Stall of a Two-Dimensional Airfoil Using an Algebraic Reynolds-Stress Turbulence Model," Centre Européen de Recherche et de Formation Avancée en Calcul Scientifique (CERFACS), TR/RF/91/52, Toulouse, France, April 1991.

[8]Rodi, W., and Scheuerer, G., "Calculation of Curved Shear Layers With Two-Equation Turbulence Models," *Physics of Fluids,* Vol. 26, No. 6, June 1983, pp. 1422–1435.

[9]Leschziner, M. A., "Numerical Implementation and Performance of Reynolds-Stress Closures in Finite-Volume Computations of Recirculating and Strongly Swirling Flows," Lecture Notes in *Introduction to the Modeling of Turbulence,* von Karman Institute for Fluid Dynamics, Brussels, March 18–21, 1991.

[10]Davidson, L., and Rizzi, A., "Navier-Stokes Computation of Airfoil in Stall Using Algebraic Reynolds-Stress Model," AIAA Paper 92-0195, Jan. 1992.

[11]Patankar, S. V., *Numerical Heat Transfer and Fluid Flow,* McGraw-Hill, New York, 1980, Chap. 5.

[12]Wolhshtein, M., "The Velocity and Temperature Distribution in One-Dimensional Flow with Turbulence Augmentation and Pressure Gradient," *International Journal of Mass and Heat Transfer,* Vol. 12, March 1969, pp. 301–318.

[13]Chen, H. C., and Patel, V. C., "Practical Near-Wall Turbulence Models for Complex Flows Including Separation," AIAA Paper 87-1300, June 1987.

[14]Palicot, L., private communication, Aerospatiale, Toulouse, France, 1990.

[15]Capbern, C., and Bonnet, C., "Opération décrochage: Rapport Final de Synthèse," Rapport Aerospatiale 443.535./89, Toulouse, France, March 1989.

[16]Gleyzes, C., "Opération décrochage: Résultats de la deuxième campagne d'essais à F2 (mesures de pression et vélocimetrie laser)," Rapport Final ONERA/CERT 57/5004.22, Toulouse, France, June 1989.

[17]Thompson, B. E., and Whitelaw, J. H., "Characteristics of a Trailing-Edge Flow With Turbulent Boundary-Layer Separation," *Journal of Fluid Mechanics,* Vol. 157, Aug. 1985, pp. 305–326.

[18]Dimitriades, K. P., and Leschziner, M. A., "A Cell-Vertex TVD Scheme for Transonic Viscous Flow," *Proceedings of the Seventh International Conference on Numerical Methods in Laminar and Turbulent Flows,* Vol. 7, Pt. 2, Stanford, CA, July 1991, pp. 874–885.

[19]Davidson, L., "Calculation of the Flow Around a High-Lift Airfoil Using an Explicit Code and an Algebraic Reynolds Stress Model, *Proceedings of the Seventh International Conference on Numerical Methods in Laminar Turbulent Flow,* Vol. 7, Pt. 2, Stanford, CA, July 1991, pp. 852–862.

Ernest V. Zoby
Associate Editor